Crossover from isotropic to directed percolation

Erwin Frey, Uwe Claus Täuber, and Franz Schwabl
Institut für Theoretische Physik, Physik-Department der Technischen Universität München, James-Franck-Strasse, D-85747 Garching, Germany
(Received 3 December 1993)

Percolation clusters are probably the simplest example for scale-invariant structures which are either governed by isotropic scaling laws ("self-similarity") or—as in the case of directed percolation—may display anisotropic scaling behavior ("self-affinity"). Taking advantage of the fact that both isotropic and directed bond percolation (with one preferred direction) may be mapped onto corresponding variants of (Reggeon) field theory, we discuss the crossover between self-similar and self-affine scaling. This has been a long-standing and yet unsolved problem because it is accompanied by different upper critical dimensions: $d_c^{\mathrm{I}} = 6$ for isotropic and $d_c^{\mathrm{D}} = 5$ for directed percolation, respectively. Using a generalized subtraction scheme we show that this crossover may nevertheless be treated consistently within the framework of renormalization group theory. We identify the corresponding crossover exponent and calculate effective exponents for different length scales and the pair correlation function to one-loop order. Thus we are able to predict at which characteristic anisotropy scale the crossover should occur. The results are subject to direct tests by both computer simulations and experiment. We emphasize the broad range of applicability of the proposed method.

PACS number(s): 05.20.−y, 05.40.+j, 64.60.Ak

I. INTRODUCTION

In describing a large variety of patterns in nature concepts from fractal geometry [1] have become of increasing importance over the past years. The simplest kind of scale invariance is *self-similarity*, i.e., invariance with respect to homogeneous dilation or contraction. A second kind of structure, which frequently appears in growth models, are *self-affine* clusters, which we define as characterized by *anisotropic scaling* (see Fig. 1).

Perhaps the most simple growth model which incorporates both of these fractal structures is percolation [2]. In ordinary percolation, sites or bonds are filled at random with probability p. The percolation process then proceeds along paths connecting occupied nearest neighbors. The clusters formed by nearest-neighbor links are self-similar, i.e., they display isotropic scaling. In directed percolation [3] the links between nearest neighbors have a bias in one preferred direction, such that the percolation process advances along this direction only. (Often this direction is referred to as the time direction t and therefore directed percolation proceeds in the direction of increasing time.) The size of the clusters in the preferred direction is characterized by a length scale different from that in the perpendicular direction. Figure 1 depicts typical clusters emerging from isotropic (a) and directed (b) percolation, respectively.

If percolation in the positive t direction is merely favored with a certain probability with respect to the negative t direction, but propagation "backward" in time is still admitted, the situation will be more complicated. If the "anisotropy" g is low, one expects almost isotropic scaling behavior in a large region of the phase diagram. However, when the critical region near the percolation threshold p_c is approached, self-affine scaling will become apparent. Similarly, if $p = p_c$, and the percolation clusters are viewed at a tiny length scale, hardly any deviations from self-similarity will be noticeable. On the other hand, if one proceeds to larger and larger scales, anisotropic scaling will become more and more important, until finally the asymptotic limit of directed percolation is reached.

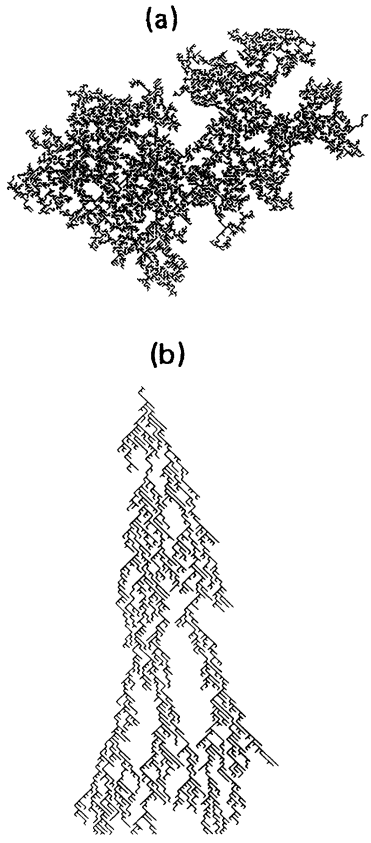

FIG. 1. Isotropic (a) and directed (b) percolation clusters.

Our aim is to provide a quantitative description of the ensuing crossover features from self-similar to self-affine scaling, when either the length scale is varied, or the threshold p_c is approached, for a biased percolation problem. More precisely, we are going to compute at which characteristic anisotropy scale g this crossover should occur, and we shall find that this crossover point depends on the specific scaling law and correspondent critical exponent under consideration. These predictions are, of course, subject to direct tests by computer simulations and/or experiments, which would thus be most desirable in order to check our results.

For the issues we have in mind, the main quantity of interest is the pair correlation function (or connectivity) $G(\mathbf{r}_2, \mathbf{r}_1)$, which measures the probability that the sites $\mathbf{r}_2$ and $\mathbf{r}_1$ are connected by some path irrespective of the other sites in the lattice. Lines of constant G hence describe the average shape of the percolating structure. In directed percolation $\mathbf{r} = (\mathbf{x}, t)$ the pair correlation function has to be causal, i.e., one has to add the restriction that $t_2 > t_1$ for G to be nonzero.

Percolation problems may be reformulated in terms of certain field theories. Cardy and Sugar [4] have shown that directed bond percolation is in the same universality class as Reggeon field theory, which has been studied intensively by particle physicists in the 1970s, below five dimensions. This universality was also confirmed numerically for $d = 2$ and $d = 3$ (see Refs. [5–7]). A corresponding mapping for isotropic site-bond correlation onto a related field-theoretical model was performed by Benzoni and Cardy [8], valid for $d < 6$ dimensions. An extension of these models to the intermediate case of anisotropic, but not entirely directed percolation is straightforward, and we shall use the ensuing field theory for our investigation of the crossover from self-similar to self-affine scaling.

The problem of directed percolation has been studied by various theoretical methods, such as high-temperature expansion for the calculation of the exponents in $d = 2$ [5], ϵ expansion [4], and Monte Carlo simulations [9, 10, 7]. The main focus of all these investigations was the determination of the independent critical exponents.

There are many processes in nature which can be described in terms of biased percolation. An example is the reaction of polymerization with the production of a giant macromolecule (gelation or vulcanization), if it occurs under anisotropic external conditions. If the seed macromolecule is washed by a flow of solution containing monomer groups, it is obvious that the probability of connection along and against the flow is different [11]. In general, directed percolation can be understood as a prototypical model for the spreading of some influence, such as transport in a strong external field [12], crack propagation [13], epidemics or forest fires with a bias [14]. One more example is the propagation of excitations in the system of neurons or neuronlike automatons.

Our paper is organized as follows. In the following section we start with an outline of the mapping of percolation problems onto "dynamical" field theories [15]. We define the specific model under consideration here and comment on the different upper critical dimensions which play a role in the limiting cases of isotropic and directed percolation, respectively. In Sec. III we shall then describe an appropriate renormalization procedure allowing for a detailed analysis of the crossover scenario. It comprises a generalization of Amit and Goldschmidt's procedure designed for bicritical points [16] enabling us to treat the fixed points with different upper critical dimension within a unified renormalization scheme. The fourth section is devoted to the solution of the renormalization group equation for the two-point vertex function and the discussion of the resulting flow equations (including their scaling behavior) for the coupling parameters in the framework of an explicit one-loop theory. On this basis, we shall identify the asymptotic critical indices for both isotropic and directed percolation, and an additional crossover exponent Δ. Finally, we shall calculate effective critical exponents for the different length scales and the wave vector dependence of the pair correlation function, which allows us to determine the relevant crossover scales. In the Appendixes, we list some technical details concerning the one-loop perturbation theory, and some properties of those integrals that emerge after the application of Feynman's parametrization, and enter the explicit expressions for the renormalization constants and flow equations.

II. MAPPING TO A FIELD-THEORETICAL MODEL

Following the considerations by Cardy and Sugar [4], and Benzoni and Cardy [8], we argue that our general percolation problem can be mapped onto a field-theoretical model. For the reader's convenience, a very brief sketch of the basic ideas entering the derivation of the probability measure is presented here; more details may be found in the literature [2, 4, 8]. As stated above, the central quantity of interest is the pair-correlation function $G^0(\mathbf{r}_2, \mathbf{r}_1)$ (we shall henceforth denote unrenormalized quantities with a superscript "0"), or probability that sites $\mathbf{r}_1 = (\mathbf{x}_1, t_1)$ and $\mathbf{r}_2 = (\mathbf{x}_2, t_2)$ belong to the same percolation cluster. In a first step, $G^0(\mathbf{r}_2, \mathbf{r}_1)$ is represented by a sum of all such graphs defined on the percolating lattice which are constructed by the following rules [2, 4, 8] (see Fig. 2).

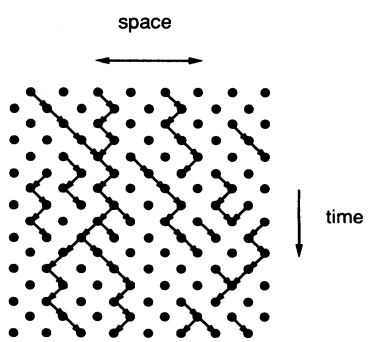

FIG. 2. Directed bonds placed on a square percolation lattice.

(1) Place oriented bonds on the lattice, in such a fashion that from each site in the diagram it is possible to reach $\mathbf{r}_2$ by following the arrows forward, and $\mathbf{r}_1$ by following the arrows backward. (2) Closed loops of arrows are not allowed. (3) Insert a factor p for each bond. (4) In order to avoid multiple countings, insert a factor $-i^n$ for each vertex where n bonds meet.

The second step is a more formal expression for $G^0(\mathbf{r}_2, \mathbf{r}_1)$, to be obtained by introducing commuting "ladder" operators $a(\mathbf{r}_i)$ and $\tilde{a}(\mathbf{r}_i)$ at each site $\mathbf{r}_i$, and an operation Tr, with the properties

$$a^2 = ia, \qquad \tilde{a}^2 = i\tilde{a}, \tag{2.1}$$

$$\mathrm{Tr}\, a = \mathrm{Tr}\, \tilde{a} = 0, \quad \mathrm{Tr}(a\tilde{a}) = 1. \tag{2.2}$$

Denoting by P an operator projecting out the graphs with closed loops, the diagrammatic rules above can now all be summarized in the formula

$$G^0(\mathbf{r}_2, \mathbf{r}_1) = \mathrm{Tr}\left(P\, a(\mathbf{r}_1) \prod_{\langle links \rangle; i,j} [1 + p\tilde{a}(\mathbf{r}_i) a(\mathbf{r}_j)] \times a(\mathbf{r}_2) \right). \tag{2.3}$$

Introducing

$$\lambda = -\ln(1-p), \tag{2.4}$$

the "transition probability" in Eq. (2.3) may be exponentiated according to

$$\prod_{\langle links \rangle; i,j} [1 + p\tilde{a}(\mathbf{r}_i) a(\mathbf{r}_j)] = \prod_{\langle links \rangle; i,j} \exp\left[\lambda \tilde{a}(\mathbf{r}_i) a(\mathbf{r}_j)\right] = \exp\left[\sum_{ij} \tilde{a}(\mathbf{r}_i) V_{ij} a(\mathbf{r}_j) \right]; \tag{2.5}$$

in the final expression here, $V_{ij} = v(\mathbf{r}_i - \mathbf{r}_j)$ is a matrix which stems from the nearest-neighbor interaction λ and depends on the details of the lattice structure, and $v(\mathbf{r})$ is a short-ranged function. The next step in our derivation is a Gaussian transformation, i.e., a representation of Eq. (2.3) by a functional integral over auxiliary fields ϕ_0 and $\tilde{\phi}_0$:

$$G^0(\mathbf{r}_2, \mathbf{r}_1) = \mathrm{Tr}\Bigg\{ P\, a(\mathbf{r}_1) \int \mathcal{D}[\phi_0] \int \mathcal{D}[\tilde{\phi}_0] \exp\left(-\sum_{i,j} \tilde{\phi}_0(\mathbf{r}_i) V_{ij}^{-1} \phi_0(\mathbf{r}_j) \right) \times \exp\left(\sum_i \left[\tilde{a}(\mathbf{r}_i)\phi_0(\mathbf{r}_i) + a(\mathbf{r}_i)\tilde{\phi}_0(\mathbf{r}_i) \right] \right) a(\mathbf{r}_2) \Bigg\}. \tag{2.6}$$

Now we take the continuum limit, and expand V_{ij}^{-1} with respect to gradients of $\mathbf{r}$; to lowest order, one has

$$v^{-1} = \frac{1}{n_c} \left(1 - s\nabla_{\mathbf{x}}^2 + r_1 \frac{\partial}{\partial t} - r_2 \frac{\partial^2}{\partial t^2} + \cdots \right), \tag{2.7}$$

where n_c is the coordination number of the lattice. Note that we have explicitly taken account of the fact that our problem displays an inversion symmetry with respect to $\mathbf{x}$; in the case of isotropic percolation the term $\propto r_1$ vanishes, and (2.7) is even invariant under transformations $t \to -t$, and hence $\mathbf{r} \to -\mathbf{r}$, while in the self-affine region the second "time" derivative becomes irrelevant.

At last, we have to perform the operation Tr in Eq. (2.6); this may be achieved by expanding the exponential with respect to powers of $a(\mathbf{r}_i)$ and $\tilde{a}(\mathbf{r}_i)$. For the detailed calculations, we refer the interested reader to the Appendix 1 of Ref. [8]. The final result for the pair correlation function is a sum over $(m+n)$-point correlation functions

$$G^0(\mathbf{x}_2, t_2; \mathbf{x}_1, t_1) = \sum_{m,n=1}^{\infty} \frac{(-i)^{m+n-2}}{m!n!} G^0_{mn}(\mathbf{x}_2, t_2; \mathbf{x}_1, t_1); \tag{2.8}$$

here the $G^0_{mn}(\mathbf{x}_2, t_2; \mathbf{x}_1, t_1)$ are defined via

$$\begin{aligned} G^0_{mn}(\mathbf{x}_2, t_2; \mathbf{x}_1, t_1) &= \langle \phi_0(\mathbf{x}_2, t_2)^m \tilde{\phi}_0(\mathbf{x}_1, t_1)^n \rangle \\ &= P \int \mathcal{D}[\phi_0] \int \mathcal{D}[\tilde{\phi}_0]\, \phi_0(\mathbf{x}_2, t_2)^m \tilde{\phi}_0(\mathbf{x}_1, t_1)^n \exp\left[\mathcal{J}[\phi_0, \tilde{\phi}_0] \right], \end{aligned} \tag{2.9}$$

where the probability measure explicitly reads

$$\mathcal{J}[\phi_0, \tilde{\phi}_0] = -\int d^D x \int dt \Bigg\{ \tilde{\phi}_0(\mathbf{x}, t) \left[r_0 - \nabla^2 - \frac{1}{c_0^2} \frac{\partial^2}{\partial t^2} + \frac{2g_0}{c_0} \frac{\partial}{\partial t} \right] \phi_0(\mathbf{x}, t) + \frac{u_0}{2} \left[\tilde{\phi}_0(\mathbf{x}, t)^2 \phi_0(\mathbf{x}, t) - \tilde{\phi}_0(\mathbf{x}, t) \phi_0(\mathbf{x}, t)^2 \right] \Bigg\}. \tag{2.10}$$

When writing down Eq. (2.10), we have omitted nonlinear terms of higher than third order with respect to the fields ϕ_0 and $\tilde{\phi}_0$ for universality (we are interested in the scaling behavior near the percolation threshold p_c) and renormalizability reasons; the neglected contributions constitute irrelevant perturbations in the sense of the renormalization group. Furthermore the expansion parameters of Eq. (2.7) have been renamed for convenience. For the percolation threshold itself one finds

$$p_c = 1 - e^{-1/n_c}, \tag{2.11}$$

and for $p \to p_c$ one has

$$r_0 \propto p - p_c. \tag{2.12}$$

In Eq. (2.9), the operator P now assures "causality," and projects out "acausal" diagrams, e.g., closed Hartree loops containing the "response" propagator (compare Ref. [15]).

On the basis of Eqs. (2.8)–(2.10) one is now in a position to construct a perturbation expansion for the pair correlation function $G^0(\mathbf{r}_2, \mathbf{r}_1)$. In this paper, however, we shall confine ourselves to the study of the renormalization-group equation for the two-point vertex function

$$\Gamma^0_{11}(\mathbf{q}, \omega) = \frac{1}{G^0_{11}(-\mathbf{q}, -\omega)}, \tag{2.13}$$

which already displays the correct scaling behavior and will permit the identification of the relevant critical exponents. Here we have defined the $(d = D+1)$-dimensional Fourier transformation according to

$$\phi_0(\mathbf{x}, t) = \int_q \int_\omega \phi_0(\mathbf{q}, \omega) e^{i(\mathbf{q}\mathbf{x} - \omega t)}, \tag{2.14}$$

where we have introduced the convenient abbreviation

$$\int_q \int_\omega \cdots = \frac{1}{(2\pi)^d} \int d^D q \int d\omega \cdots . \tag{2.15}$$

For the renormalization of the nonlinear coupling u_0, we shall also have to consider the two three-point vertex functions

$$\Gamma^0_{12}\left(-\mathbf{q}, -\omega; \frac{\mathbf{q}}{2}, \frac{\omega}{2}; \frac{\mathbf{q}}{2}, \frac{\omega}{2}\right) = -\frac{G^0_{21}\left(-\frac{\mathbf{q}}{2}, -\frac{\omega}{2}; -\frac{\mathbf{q}}{2}, -\frac{\omega}{2}; \mathbf{q}, \omega\right)}{G^0_{11}(\mathbf{q}, \omega) G^0_{11}(\frac{\mathbf{q}}{2}, \frac{\omega}{2})^2}, \tag{2.16}$$

$$\Gamma^0_{21}\left(\frac{\mathbf{q}}{2}, \frac{\omega}{2}; \frac{\mathbf{q}}{2}, \frac{\omega}{2}; -\mathbf{q}, -\omega\right) = -\frac{G^0_{12}\left(\mathbf{q}, \omega; -\frac{\mathbf{q}}{2}, -\frac{\omega}{2}; -\frac{\mathbf{q}}{2}, -\frac{\omega}{2}\right)}{G^0_{11}(\mathbf{q}, \omega) G^0_{11}(\frac{\mathbf{q}}{2}, \frac{\omega}{2})^2}. \tag{2.17}$$

The practical advantage of using these vertex functions instead of the correlation functions themselves is their correspondence to the one-particle irreducible diagrams within the graphical representation in terms of Feynman diagrams (see, e.g., Ref. [17]). (We remark that in the definitions of the vertex functions (2.13), (2.16), and (2.17), the Dirac δ functions stemming from translational symmetry in $\mathbf{x}$ and t have been split off.)

Returning to the "dynamical" functional [15] (2.10), it is easily seen that setting the parameter g_0 to zero leads to the field-theoretical model of Benzoni and Cardy for the special case of isotropic bond percolation in $d = D+1$ dimensions [8]. Of course, c_0 may then be assumed to take the value 1. On the other hand, in the limit $g_0 \to \infty$ and $c_0 \to \infty$ such that g_0/c_0 remains finite, one obtains Cardy and Sugar's Reggeon field theory for the problem of directed percolation with t denoting the preferred direction [4]. Any finite value of g_0 hence corresponds to a biased percolation problem, with g_0 characterizing the strength of the inherent anisotropy.

We now proceed with a simple dimensional analysis to determine the upper critical dimensions of our model in the different limiting cases. If we define

$$[x] = [t] = \Lambda^{-1}, \tag{2.18}$$

where Λ is a cutoff wave vector which defines the microscopic length scale of the problem, then we find for the primitive dimension of the stochastic fields (using $[J] = \Lambda^0$)

$$[\phi_0(\mathbf{x}, t)] = [\tilde{\phi}_0(\mathbf{x}, t)] = \Lambda^{(2-d)/2}. \tag{2.19}$$

Hence the coupling parameters acquire the following "naive" dimensions:

$$[r_0] = \Lambda^2, \quad [c_0] = \Lambda^0, \quad [g_0] = \Lambda^1,$$

$$\text{and} \quad [u_0] = \Lambda^{(d-6)/2}. \tag{2.20}$$

The upper critical dimension may be identified by noting that the relevant nonlinear coupling has zero primitive dimension at $d = d_c$. In the isotropic case ($g_0 = 0$), the expansion parameter of the perturbation series turns out to be $u_0^2 c_0$, and hence the upper critical dimension for isotropic percolation is found to be $d_c^{\mathrm{I}} = 6$. In the extremely anisotropic limit ($g_0 \to \infty$ and $g_0/c_0 = \text{const}$) on the other hand, a simple rescaling of the fields shows that now the effective coupling is $u_0^2 c_0/g_0$, and using Eq. (2.20) demonstrates that $d_c^{\mathrm{D}} = 5$ for directed percolation. Hence accompanying the crossover from self-similar to self-affine scaling, there is a change of the upper critical dimension. At first sight, this renders this crossover problem rather cumbersome, at least if one wants to use an $(\epsilon = d_c - d)$ expansion near d_c. We shall see, however, that a procedure similar to Amit and Goldschmidt's treatment of bicritical points [16] will enable us to give a consistent mathematical description of this crossover. Of course, we shall have to refrain from any ϵ expansion. We would like to remark that different modifications of this (somewhat misleadingly) so-called "generalized minimal subtraction scheme" have been successfully employed by Lawrie [18] and the present authors [19–21] for further interesting crossover scenarios.

III. PERTURBATION THEORY AND RENORMALIZATION

On the basis of Eq. (2.10), one may derive the perturbation series with respect to u_0 following the common procedure (see, e.g., Ref. [17]). From the bilinear part of the "dynamic" functional $\mathcal{J}[\phi_0, \tilde{\phi}_0]$, one easily derives the free propagator

$$G^0_{11\,(0)}(\mathbf{q}, \omega) = \frac{1}{r_0 + q^2 + \omega^2/c_0^2 - 2i\omega g_0/c_0}, \tag{3.1}$$

and the vertices may be read off from the anharmonic part of (2.10). In Fig. 3, we depict these elements for constructing the Feynman graphs of our field-theoretical representation of the biased percolation problem.

For $r_0 \to 0$, the ensuing perturbation theory is of course infrared divergent, leading to nontrivial critical exponents. These anomalous dimensions are derived via studying the ultraviolet singularities of the field theory, which appear at the upper critical dimension d_c, when the momentum cutoff Λ is pushed to infinity (see, e.g., Ref. [17]). Finite values are then assigned to these UV-divergent integrals through the application of a regularization prescription. We shall choose the dimensional regularization scheme as introduced by t'Hooft and Veltman [22]; here the $(\Lambda \to \infty)$ singularities appear as poles $\propto 1/(d_c - d)$.

The ultraviolet divergences may then be collected in renormalization constants and absorbed into the definition of multiplicatively renormalized quantities. Thus we define the renormalized fields

$$\phi = Z_\phi^{1/2}\phi_0, \qquad \tilde{\phi} = Z_\phi^{1/2}\tilde{\phi}_0, \tag{3.2}$$

and the renormalized parameters

$$r = Z_\phi^{-1} Z_r (r_0 - r_{0c})\mu^{-2}, \tag{3.3}$$

$$c^2 = Z_\phi Z_c^{-1} c_0^2, \tag{3.4}$$

$$g = Z_\phi^{-1/2} Z_c^{-1/2} Z_g g_0 \mu^{-1}, \tag{3.5}$$

$$u = Z_\phi^{-3/2} Z_u u_0 B_d^{1/2} \mu^{(d-6)/2}. \tag{3.6}$$

Note that both fields are renormalized with the same Z factor, implying that $\Gamma_{11} = Z_\phi^{-1}\Gamma^0_{11}$, $\Gamma_{12} = Z_\phi^{-3/2}\Gamma^0_{12}$, and $\Gamma_{21} = Z_\phi^{-3/2}\Gamma^0_{21}$.

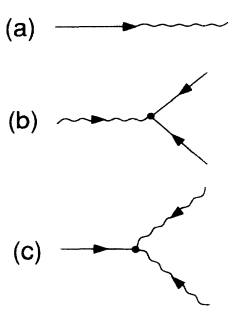

FIG. 3. Propagator and vertices of the field-theoretical representation used in the text.

In (3.3) we have taken into account the fact that the fluctuations will also shift the percolation threshold. Furthermore we have rendered the renormalized quantities dimensionless by introducing the explicit arbitrary length scale $1/\mu$, and have finally included the geometric factor

$$B_d = \frac{\Gamma(4 - d/2)}{(4\pi)^{d/2}} \tag{3.7}$$

in the definition of the renormalized coupling (3.6).

In the case of crossover phenomena, however, there is (at least) one additional relevant length scale besides the correlation length, given by an anisotropy or "mass" parameter describing the variation from one scaling region to the other. This implies the technical difficulty that both the UV and IR singularities will differ in the two distinct scaling regimes. In the "traditional" approach to crossover problems, one would compute the critical exponents in the vicinity of one of the stable fixed points; all the crossover features would then be contained in the accompanying scaling function as corrections to this scaling behavior. However, in general a calculation to high order in the perturbation expansion would be required in order to achieve a satisfactory description of the entire crossover region. Of course, using an $(\epsilon = d_c - d)$ expansion with respect to either of the fixed points renders the other one completely inaccessible, if their upper critical dimensions do not coincide. Therefore Amit and Goldschmidt's idea to incorporate the crossover features already in the exponent functions has proven much more successful than treating the problem on the basis of scaling functions. The essential prescription one has to bear in mind is that the renormalization constants are not solely functions of the anharmonic coupling, but necessarily also of the additional "mass" or anisotropy parameter describing the interplay between the two different scaling regimes [16].

In our case this second length scale is related to the anisotropy parameter g_0. For a consistent treatment of the entire crossover region, one thus has to assure that the UV singularities are absorbed into the Z factors for any arbitrary value of g_0, including $g_0 \to \infty$. This is not a trivial prescription, as usually the $1/(d_c - d)$ poles will be altered in the different scaling regimes. For the situation that we have in mind, even the value of the upper critical dimension is bound to change as the crossover takes place, in contrast to previously studied cases [18–21]. However, we shall demonstrate that with the above stated so-called "generalized subtraction scheme" this change in the upper critical dimension may be incorporated into the usual formalism without any drastic changes, if one refrains from any ϵ expansion about d_c. The perturbation series is then an expansion with respect to the effective coupling v to be introduced later, which is not an *a priori* small parameter, and the perturbation expansion is uncontrolled in this sense [23]. If higher orders of the perturbation expansion were known, one could substantially refine the theory by a Borel resummation procedure. For a more detailed discussion of the question in which cases one may dispense with a $(d_c - d)$ expansion, we refer to work of Schloms and Dohm [24].

Another (minor) price to be paid is that for the flow equations and related quantities only numerical solutions are accessible, and merely the limiting cases of $g_0 = 0$ and $g_0 \to \infty$, respectively, allow for an analytical investigation. We remark that the somewhat misleading term "generalized subtraction scheme" stems from the fact that in the framework of an ϵ expansion this corresponds to adding logarithms of g_0, which are finite in the limit $\epsilon \to 0$, to the Z factors; see the original work by Amit and Goldschmidt [16]. It should be emphasized that the procedure described here is obviously applicable to a great variety of crossover problems (for some examples see Sec. V).

After these general statements, let us return to our explicit calculations. In Fig. 4 we have depicted the one-loop diagrams for Γ^0_{11}, Γ^0_{12}, and Γ^0_{21}. From $\partial_{q^2}\Gamma_{11}(\mathbf{q},0)\,|_{q=0}$ one infers directly the field renormalization Z_ϕ, while Z_r, Z_c, and Z_g can be calculated by investigation of $\Gamma_{11}(0,0)$, $\partial_{\omega^2}\Gamma_{11}(0,\omega)\,|_{\omega=0}$, and $\partial_\omega\Gamma_{11}(0,\omega)\,|_{\omega=0}$, respectively. Finally Z_u is to be obtained from one of the renormalized three-point vertex functions at vanishing external momenta and frequencies (see Appendix A). All these vertex functions are investigated at finite "mass" $r_0 = \mu^2$, in order to avoid complications stemming from additional infrared singularities. Thus the renormalization scale μ comes into play.

The explicit one-loop results for the renormalization factors—being functions of the anisotropy scale g_0—read

$$Z_\phi = 1 - \frac{u_0^2 c_0 B_d \mu^{d-6}}{8(6-d)}\left[I^d_{15}(g_0/\mu) - I^d_{33}(g_0/\mu)\right], \tag{3.8}$$

$$Z_r = 1 - \frac{u_0^2 c_0 B_d \mu^{d-6}}{2(6-d)} I^d_{15}(g_0/\mu), \tag{3.9}$$

$$Z_c = 1 - \frac{u_0^2 c_0 B_d \mu^{d-6}}{8(6-d)}\left[I^d_{15}(g_0/\mu) - I^d_{33}(g_0/\mu)\right] + \frac{u_0^2 c_0 g_0^2 B_d \mu^{d-8}}{8}\left[2I^d_{35}(g_0/\mu) - I^d_{53}(g_0/\mu)\right], \tag{3.10}$$

$$Z_g = 1 - \frac{u_0^2 c_0 B_d \mu^{d-6}}{4(6-d)}\left[I^d_{15}(g_0/\mu) - I^d_{33}(g_0/\mu)\right], \tag{3.11}$$

$$Z_u = 1 - \frac{u_0^2 c_0 B_d \mu^{d-6}}{6-d} I^d_{15}(g_0/\mu), \tag{3.12}$$

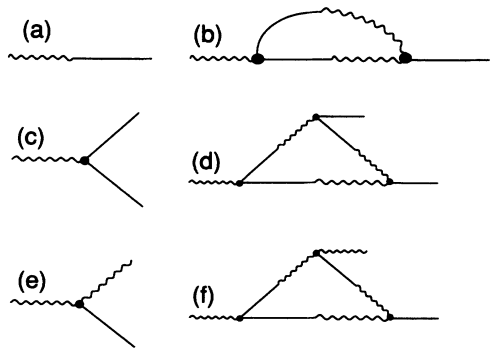

FIG. 4. One-loop diagrams for (a),(b) Γ^0_{11}, (c),(d) Γ^0_{12}, and (e),(f) Γ^0_{21}.

where we have introduced the abbreviations $I^d_{mn}(g_0/\mu)$ for a certain class of Feynman parameter integrals which appear in the course of the calculations (compare Appendix B).

At this point, we may study the behavior of the Z factors in the two limiting cases of isotropic and directed percolation, respectively. Let us investigate Z_u, for example; for $g_0 = 0$ we find with Eq. (B3)

$$g_0 = 0: \qquad Z_u = 1 - \frac{2u_0^2 c_0 B_d \mu^{d-6}}{6-d}, \tag{3.13}$$

while in the opposite case $g_0 \to \infty$ the pole at $d = 6$ is cancelled and replaced by another one at $d = 5$

$$g_0 \to \infty: \qquad Z_u = 1 - \frac{u_0^2 c_0 B_d B(1/2,(7-d)/2)\mu^{d-5}}{g_0(5-d)} \tag{3.14}$$

[here Eq. (B4) has been used]. Hence our prescription provides the relevant effective coupling constants and the correct pole structure in both limits, and interpolates smoothly in between.

Finally the fluctuation-induced shift of the percolation threshold results as the solution of the implicit equation

$$r_{0c} = \left[\frac{u_0^2 c_0 B_d}{(d-4)(6-d)} I^d_{13}(g_0/\sqrt{r_{0c}})\right]^{2/(6-d)}. \tag{3.15}$$

Note that r_{0c} is a nonanalytical function of u_0 for both limits $g_0 = 0$ and $g_0 \to \infty$ (see, e.g., Ref. [24]).

IV. RENORMALIZATION-GROUP AND FLOW EQUATIONS

A. Scaling behavior and critical exponents

The renormalization-group equation serves to connect the asymptotic theory, where the infrared singularities manifest themselves, with a region in parameter space, where the coupling u is finite (but not necessarily small) and ordinary "naive" perturbation expansion becomes applicable. It explicitly takes advantage of the scale invariance of the system near a critical point (i.e., the percolation threshold in our case). More precisely, we observe that the bare two-point vertex function is of course independent of the arbitrary renormalization scale μ:

$$\mu\frac{d}{d\mu}\bigg|_0 \Gamma^0_{11}(r_0, c_0, g_0, u_0, \mathbf{q}, \omega) = 0. \tag{4.1}$$

Introducing Wilson's flow functions

$$\zeta_\phi = \mu\frac{\partial}{\partial\mu}\bigg|_0 \ln Z_\phi, \tag{4.2}$$

$$\zeta_r = \mu\frac{\partial}{\partial\mu}\bigg|_0 \ln\frac{r}{r_0 - r_{0c}} = -2 - \zeta_\phi + \mu\frac{\partial}{\partial\mu}\bigg|_0 \ln Z_r, \tag{4.3}$$

$$\zeta_c = \mu\frac{\partial}{\partial\mu}\bigg|_0 \ln\frac{c}{c_0} = \frac{1}{2}\zeta_\phi - \frac{1}{2}\mu\frac{\partial}{\partial\mu}\bigg|_0 \ln Z_c, \tag{4.4}$$

$$\zeta_g = \mu\frac{\partial}{\partial\mu}\bigg|_0 \ln\frac{g}{g_0} = -1 - \zeta_\phi + \zeta_c + \mu\frac{\partial}{\partial\mu}\bigg|_0 \ln Z_g, \tag{4.5}$$

$$\zeta_u = \mu\frac{\partial}{\partial\mu}\bigg|_0 \ln\frac{u}{u_0} = \frac{d-6}{2} - \frac{3}{2}\zeta_\phi + \mu\frac{\partial}{\partial\mu}\bigg|_0 \ln Z_u, \quad (4.6)$$

we may transform Eq. (4.1) into a partial differential equation for the renormalized vertex function

$$\left[\mu\frac{\partial}{\partial\mu} + \zeta_r r\frac{\partial}{\partial r} + \zeta_c c\frac{\partial}{\partial c} + \zeta_g g\frac{\partial}{\partial g} + \zeta_u u\frac{\partial}{\partial u} + \zeta_\phi\right] \times\Gamma_{11}(\mu, r, c, g, u, \mathbf{q}, \omega) = 0. \quad (4.7)$$

The symbol $|_0$ indicates that all the derivatives are to be taken at fixed bare parameters r_0, g_0, and u_0. One should note that, as a consequence of the generalized renormalization scheme, all the flow functions ζ are functions of u, c, *and* g.

The renormalization-group equation (4.7) is now readily solved with the method of characteristics. The characteristics $a(\ell)$ of Eq. (4.7) define the running parameters and coupling constants into which these transform when $\mu \to \mu(\ell) = \mu\ell$. They are given by the solutions to first-order differential equations ($a = r, c, g, u$)

$$\ell\frac{da(\ell)}{d\ell} = \zeta_a(\ell)a(\ell), \quad (4.8)$$

with the initial conditions $r(1) = r$, $c(1) = c$, $g(1) = g$, and $u(1) = u$, namely

$$a(\ell) = a e^{\int_1^\ell \zeta_a(\ell')d\ell'/\ell'}. \quad (4.9)$$

Defining the dimensionless vertex function $\hat{\Gamma}_{11}$ according to

$$\Gamma_{11}(\mu, r, c, g, u, \mathbf{q}, \omega) = \mu^2\hat{\Gamma}_{11}\left(r, v, \frac{\mathbf{q}}{\mu}, \frac{g\omega}{c\mu}, \frac{\omega^2}{c^2\mu^2}\right), \quad (4.10)$$

the solution of (4.7) reads

$$\Gamma_{11}(\mu, r, c, g, u, \mathbf{q}, \omega) = \mu^2\ell^2 e^{\int_1^\ell \zeta_\phi(\ell')d\ell'/\ell'} \times\Gamma_{11}\left(r(\ell), v(\ell), \frac{\mathbf{q}}{\mu\ell}, \frac{g(\ell)\omega}{c(\ell)\mu\ell}, \frac{\omega^2}{c(\ell)^2\mu^2\ell^2}\right). \quad (4.11)$$

Here we have introduced an effective anharmonic coupling

$$v = u^2 c I_{17}^d(g), \quad (4.12)$$

which acquires finite values in both limits, $g \to 0$ and $g \to \infty$. Defining the corresponding β function

$$\beta_v = \mu\frac{\partial}{\partial\mu}\bigg|_0 v, \quad (4.13)$$

the flow of the running coupling $v(\ell)$ is given by the differential equation

$$\ell\frac{dv(\ell)}{d\ell} = \beta_v(\ell). \quad (4.14)$$

In the flow equations above, the parameter ℓ may be considered as describing the effect of a scaling transformation upon the system. Obviously, the theory becomes scale invariant when a fixed-point v^*, to be obtained as a zero of the β function,

$$\beta_v(v^*) = 0, \quad (4.15)$$

is approached. The properties of Γ_{11} in the vicinity of the fixed point will yield the correct asymptotic behavior, if the latter is infrared stable, i.e., if $\partial\beta_v/\partial v|_{v=v^*} > 0$ is satisfied, for in this case the flow of the running coupling will reach v^* for $\ell \to 0$.

We now turn to the investigation of (4.11) near a fixed point v^*; introducing the fixed-point values of the ζ functions $\zeta_a^* = \zeta_a(v = v^*)$, also called the anomalous dimensions of the parameters a, we find that Γ_{11} becomes a generalized homogeneous function

$$\Gamma_{11}(\mu, r, c, g, u, \mathbf{q}, \omega) = \mu^2\ell^{2+\zeta_\phi^*}\hat{\Gamma}_{11}\left(r\ell^{\zeta_r^*}, v^*, \frac{\mathbf{q}}{\mu\ell}, \frac{g\omega}{c\mu\ell^{1+\zeta_c^*-\zeta_g^*}}, \frac{\omega^2}{c^2\mu^2\ell^{2(1+\zeta_c^*)}}\right). \quad (4.16)$$

Using the matching condition $\ell = q/\mu$, one arrives at the following general *self-affine* scaling form:

$$\Gamma_{11}(\mu, r, c, g, u, \mathbf{q}, \omega) \propto q^{2-\eta_\perp}\hat{\Gamma}_{11}\left(\frac{r}{(q/\mu)^{1/\nu_\perp}}, v^*, 1, \frac{g\omega}{c\mu(q/\mu)^z}, \frac{\omega^2}{c^2\mu^2(q/\mu)^{2z(1-\Delta)}}\right), \quad (4.17)$$

where we have defined *four* independent critical exponents according to

$$\eta_\perp = -\zeta_\phi^*, \quad \nu_\perp = -\frac{1}{\zeta_r^*}, \quad z = 1 + \zeta_c^* - \zeta_g^*, \quad \text{and} \quad z\Delta = -\zeta_g^*. \quad (4.18)$$

$\eta_\perp$ and $\nu_\perp$ correspond to the two independent indices familiar from the theory of static critical phenomena. The exponent z was introduced in analogy to a dynamical critical exponent, and is in our case related to the anisotropic scaling behavior [25]. Finally, Δ is a crossover exponent, $0 < \Delta < 1$, describing the transition from isotropic to directed percolation. It stems from the fact that there appear *two* different scaling variables for the "frequency" ω in Eq. (4.17). In the asymptotic limit of directed percolation, $g \to \infty$ (accompanied by $c \to \infty$ while g/c remains finite), the second scaling variable vanishes, and the scaling behavior is described by the *three* exponents $\eta_\perp$, $\nu_\perp$, and z.

Similarly, with the choice $\ell = (g\omega/c\mu)^{1/(1+\zeta_c^*-\zeta_g^*)}$ Eq. (4.16) reads

$$\Gamma_{11}(\mu,r,c,g,u,\mathbf{q},\omega) \propto \omega^{2-\eta_\parallel}\hat{\Gamma}_{11}\left(\frac{r}{(q/\mu)^{1/\nu_\parallel}}, v^*, \frac{q}{\mu(g\omega/c\mu)^{1/z}}, 1, \frac{\omega^2}{c^2\mu^2(g\omega/c\mu)^{2(1-\Delta)}}\right), \tag{4.19}$$

where [25]

$$2-\eta_\parallel = (2-\eta_\perp)/z, \quad \text{and} \quad \nu_\parallel = z\nu_\perp. \tag{4.20}$$

Moreover, $\ell = r^{-1/\zeta_r^*}$ leads to

$$\Gamma_{11}(\mu,r,c,g,u,\mathbf{q},\omega) \propto r^\gamma\hat{\Gamma}_{11}\left(1, v^*, \frac{q}{\mu}r^{-\nu_\perp}, \frac{g\omega}{c\mu}r^{-\nu_\parallel}, \frac{\omega^2}{c^2\mu^2}r^{-2\nu_\parallel(1-\Delta)}\right), \tag{4.21}$$

with another ("static") exponent γ, related to $\nu_\perp$ and $\nu_\parallel$ via

$$\gamma = \nu_\perp(2-\eta_\perp) = \nu_\parallel(2-\eta_\parallel). \tag{4.22}$$

For the sake of completeness, we finally state the scaling relations [3]

$$2\beta+\gamma = 2-\alpha = D\nu_\perp+\nu_\parallel = 2\beta\delta-\gamma = \beta(1+\delta) \tag{4.23}$$

for exponents α, β, and δ, to be defined in just the same way as for ordinary continuous phase transitions [17].

In the special case of isotropic percolation ($g_0 = 0$), the scaling relations become considerably simpler. For example, instead of Eq. (4.21) one finds *self-similar* behavior according to

$$\Gamma_{11}(\mu,r,c,0,u,\mathbf{q},\omega) \propto r^\gamma\hat{\Gamma}_{11}\left(1, v^*, \frac{q}{\mu}r^{-\nu}, 0, \frac{\omega^2}{c^2\mu^2}r^{-2\nu}\right), \tag{4.24}$$

with *two* independent critical exponents $\eta = -\zeta_\phi^*$ and $\nu = -1/\zeta_r^*$. The scaling relations reduce to $\gamma = \nu(2-\eta)$ and $2\beta+\gamma = 2-\alpha = d\nu$. On leaving the self-similar scaling region, a second scaling variable comes into play, leading to the appearance of the crossover exponent Δ defined above [Eqs. (4.17), (4.19), and (4.21)], and eventually to anisotropic scaling.

B. One-loop results

To one-loop order, Wilson's functions as derived from Eqs. (4.2) – (4.6) and (3.8) – (3.12) read

$$\zeta_\phi = \frac{v}{8}\left[1-\frac{I_{35}^d(g)}{I_{17}^d(g)}\right], \tag{4.25}$$

$$\zeta_r = -2+\frac{3v}{8}+\frac{v}{8}\frac{I_{35}^d(g)}{I_{17}^d(g)}, \tag{4.26}$$

$$\zeta_c = -\frac{vg^2(d-8)}{16}\left[2\frac{I_{37}^d(g)}{I_{17}^d(g)}-\frac{I_{55}^d(g)}{I_{17}^d(g)}\right], \tag{4.27}$$

$$\zeta_g = -1+\frac{v}{8}\left[1-\frac{I_{35}^d(g)}{I_{17}^d(g)}\right] - \frac{vg^2(d-8)}{16}\left[2\frac{I_{37}^d(g)}{I_{17}^d(g)}-\frac{I_{55}^d(g)}{I_{17}^d(g)}\right], \tag{4.28}$$

$$\zeta_u = \frac{d-6}{2}+\frac{13v}{16}+\frac{3v}{16}\frac{I_{35}^d(g)}{I_{17}^d(g)}, \tag{4.29}$$

[here Eqs. (B5) and (B6) of Appendix B have been applied].

In the following two special situations, we may explicitly evaluate these general relations: In the case $g \to 0$, we find $v \to 2u^2c$ [using (B3)]; thus

$$g \to 0: \qquad \beta_v = v\left(d-6+\frac{7}{4}v\right), \tag{4.30}$$

with the stable fixed point of isotropic percolation (for $d<6$)

$$v_I^* = \frac{4}{7}(6-d). \tag{4.31}$$

The fixed-point values for the ζ functions are $\zeta_\phi^* = v^*/12$, $\zeta_r^* = -2+5v^*/12$, $\zeta_c^* = 0$, and $\zeta_g^* = -1+v^*/12$. Hence we find the following isotropic critical exponents [$\eta = \eta_\perp(v_I^*)$ and $\nu = \nu_\perp(v_I^*)$]:

$$\eta = -\frac{6-d}{21} \quad \text{and} \quad \nu^{-1} = 2-\frac{5(6-d)}{21}. \tag{4.32}$$

In Eq. (4.17), the term linear in ω vanishes for $g \to 0$, and inserting $\zeta_c^* = 0$ yields

$$z(1-\Delta) = 1, \tag{4.33}$$

which is equivalent to isotropic scaling in $d = D+1$ dimensions; compare (4.24). The crossover exponent

$$\Delta = \frac{1-(6-d)/21}{2-(6-d)/21} \tag{4.34}$$

provides the power law according to which the isotropic scaling region is left in favor of the anisotropic behavior to be discussed below. For $d>6$, the isotropic Gaussian fixed point

$$v_{GI}^* = 0 \tag{4.35}$$

is stable, with the corresponding mean-field exponents

$$\eta_\perp = 0, \quad \nu_\perp = \frac{1}{2}, \quad z = 2, \quad \text{and} \quad \Delta = \frac{1}{2}. \tag{4.36}$$

The limit of directed percolation is characterized by a diverging anisotropy scale $g \to \infty$. Using Eq. (B4), the coupling parameter becomes $v \to u^2cB(1/2,(7-d)/2)/g$ (note the additional factor $1/g$), and the β function now reads

$$g \to \infty : \qquad \beta_v = v\left(d - 5 + \frac{3}{2}v\right). \tag{4.37}$$

Therefore, for $d > 5$ the directed Gaussian fixed point

$$v^*_{\mathrm{GD}} = 0 \tag{4.38}$$

becomes stable, which again leads to the exponents of Eq. (4.36).

On the other hand, for dimensions $d < 5$ the asymptotic behavior is governed by the nontrivial anisotropic scaling fixed point

$$v^*_{\mathrm{D}} = \frac{2}{3}(5 - d). \tag{4.39}$$

Note that the upper critical dimension has changed to $d_c^{\mathrm{D}} = 5$, in contrast to the isotropic case, where $d_c^{\mathrm{I}} = 6$; physically, this reduction is due to the suppression of fluctuations by the anisotropy, and may be formally traced back to the appearance of the factor $1/g$ in the expression for the asymptotic coupling. Inserting (4.39) into the results for the ζ functions, $\zeta^*_\phi = v^*/8$, $\zeta^*_r = -2 + 3v^*/8$, $\zeta^*_c = v^*/8$, and $\zeta^*_g = -1 + v^*/4$, we find the following critical indices:

$$\eta_\perp = -\frac{5-d}{12}, \quad \nu_\perp^{-1} = 2 - \frac{5-d}{4}, \quad z = 2 - \frac{5-d}{12},$$

$$\text{and} \quad z\Delta = 1 - \frac{5-d}{6}, \tag{4.40}$$

which characterize the self-affine scaling of the percolation clusters with preferred "time" direction [4]. The anisotropy is reflected in the exponent z, and Δ now describes the crossover from isotropic to directed percolation near the anisotropic percolation fixed point v^*_{D}. We have collected the four fixed points and the corresponding values for the independent critical exponents in Table I.

Thus we have demonstrated that both the self-similar and the self-affine scaling behavior are within the scope of the present theory, at least for dimensions $d \leq 5$; for $5 < d \leq 6$ the model is not renormalizable in the directed limit, and the crossover description based on extracting the UV poles may be questionable. However, in this case the asymptotics of the model are simply described by the mean-field exponents corresponding to the Gaussian fixed point v^*_{GD}, with logarithmic corrections for $d = 5$, and at least the qualitative features of the crossover to this Gaussian theory are well reproduced by our formalism (see also Refs. [19] and [21]). At any rate, this discussion again emphasizes the fact that no expansion with respect to a *fixed* upper critical dimension can be applied consistently [from our procedure a kind of "effective upper critical dimension" $d_c(g)$, varying with the anisotropy scale g, might be extracted].

For the physically interesting situation $d < 5$, note that a smooth interpolation between the two asymptotic cases is obtained at every stage of the present theory, i.e., for the renormalization constants, the ζ and β functions, the fixed-point values, and the scaling functions. We shall now proceed to study the entire crossover region between these asymptotic regimes, which can be readily done by solving the coupled set of flow equations (4.8) with (4.25)–(4.29) numerically.

We start with the analysis of the flow diagram for the effective coupling "constants" $v(\ell)$ and $\tilde{g}(\ell) = g(\ell)/[1 + g(\ell)]$ (the latter assumes values in the interval $[0, 1]$ only, which is more convenient than the range $[0, \infty]$ of the original anisotropy parameter g), shown in Fig. 5. The four fixed points, as summarized in Table I, namely those for isotropic percolation (I), directed percolation (D), Gaussian isotropic (GI), and Gaussian directed (GD) percolation, respectively, determine the topology of the $(v, \tilde{g})$ flow diagram (where we have chosen $d = 3$ and $\mu = 1$ for the renormalization scale.) The only infrared-stable fixed point is the one for directed percolation, $(v^*, \tilde{g}^*) = (\frac{2}{3}(5 - d), 1)$. All other fixed points are unstable, but as can be inferred from Fig. 5, they are more or less attractive depending on the initial value for the coupling constants. The flow diagram is divided into two regions by a separatrix, which constitutes the renormalization-group trajectory from the fixed point v^*_{I} to v^*_{D}, describing the universal crossover from self-similar to self-affine scaling. For initial values $v \leq v_{\mathrm{I}}$, there are besides the stable fixed point for directed percolation three unstable fixed points (I), (GI), and (GD). Starting from the Gaussian isotropic fixed point (GI), the renormalization-group trajectories traverse regions close to the fixed points (I) or (GD), depending on the initial values $\tilde{g}(1)$ and $v(1)$, before they finally reach the infrared-stable fixed point for directed percolation (D). The competition between all these fixed points will also become apparent in the flow of the effective exponents (e.g., for the pair correlation function). For initial values $v \geq v^*_{\mathrm{I}}$ there is only one relevant unstable fixed point (I).

TABLE I. Fixed point values for the effective coupling "constants" $v(\ell)$ and $\tilde{g}(\ell)$ at the isotropic (I), Gaussian isotropic (GI), directed (D), and Gaussian directed (GD) fixed points and the corresponding values of the four independent critical exponents. The other critical indices may be inferred from scaling relations [see Eqs. (4.20), (4.22), and (4.23)].

Fixed point	v^*	$\tilde{g}^*$	$\eta_\perp$	$\nu_\perp^{-1}$	z	Δ
GI	0	0	0	2	2	$\frac{1}{2}$
I	$\frac{4}{7}(6-d)$	0	$-\frac{6-d}{21}$	$2 - \frac{5(6-d)}{21}$	$2 - \frac{6-d}{21}$	$\frac{1-(6-d)/21}{2-(6-d)/21}$
GD	0	1	0	2	2	$\frac{1}{2}$
D	$\frac{2}{3}(5-d)$	1	$-\frac{5-d}{12}$	$2 - \frac{5-d}{4}$	$2 - \frac{5-d}{12}$	$\frac{1-(5-d)/6}{2-(5-d)/12}$

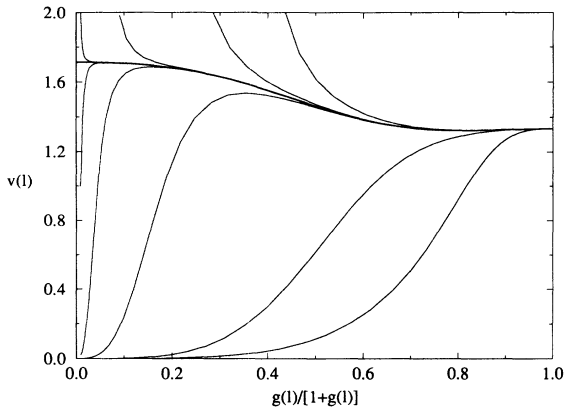

FIG. 5. Renormalization-group trajectories in the $(v, \tilde{g})$ parameter space for the crossover from isotropic to directed percolation (to one-loop order) in $d = D + 1 = 3$ dimensions. In order to map the range $[0, \infty]$ of g onto the interval $[0, 1]$, we use the variable $\tilde{g} = g/(1 + g)$ instead of the anisotropy parameter g.

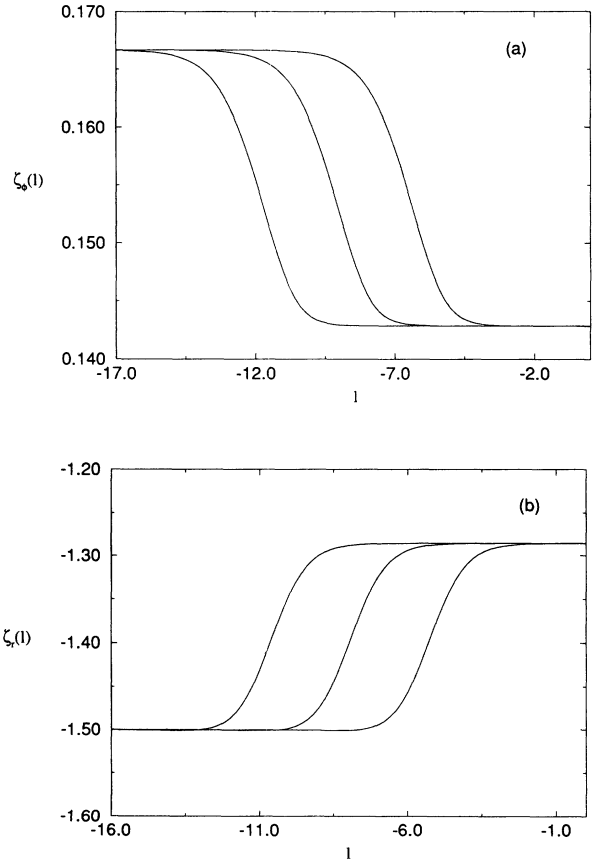

FIG. 6. Flow dependence of $\zeta_\phi(\ell)$ (a) and $\zeta_r(\ell)$ (b), where we have chosen a fixed initial value $v(1) = v_I^*$ for the three-point coupling and a series of initial values for the anisotropy parameter $[g(1) = 10^{-2}, 10^{-3}, \text{and } 10^{-4}]$.

As a result of the flow dependence of the coupling constants also the ζ functions, whose fixed-point values are related to the critical exponents, display crossover behavior. In Fig. 6 we exemplify this flow dependence for the ζ functions $\zeta_\phi(\ell)$ and $\zeta_r(\ell)$, respectively, where we have chosen a fixed initial value $v(1) = v_I^*$ for the three-point coupling, and a series of initial values for the anisotropy parameter $[g(1) = 10^{-2}, 10^{-3}, \text{and } 10^{-4}]$.

The most important conclusion to be drawn from the crossover behavior of the ζ functions is that the crossover for the anomalous dimension of the stochastic fields ζ_ϕ starts at values of the flow parameter which are approximately one order of magnitude smaller than the corresponding values for ζ_r. This should then also be visible as different crossover locations for the distinct effective exponents of the connectivity G.

C. Effective exponents for the pair correlation function

In this paragraph we consider the effects of the crossover on the most interesting physical quantity, namely the pair correlation function. As discussed in Sec. II, the scaling behavior of the connectivity is identical to that of the two-point function $G_{11}(\mathbf{q}, \omega) = \Gamma_{11}(-\mathbf{q}, -\omega)^{-1}$, which has been studied in the preceding subsection.

As a first approximation, one can use the zero-loop result for the scaling function and find

$$\Gamma_{11}(r, \mathbf{q}, \omega) = \mu^2 \ell^2 e^{\int_1^\ell \zeta_\phi(\ell')d\ell'/\ell'} \left[r(\ell) + \frac{q^2}{\mu^2 \ell^2} + \frac{\omega^2}{\mu^2 \ell^2 c(\ell)^2} + 2i \frac{\omega g(\ell)}{\mu \ell c(\ell)} \right]. \tag{4.41}$$

It is quite straightforward to calculate corrections to this zero-loop result for the scaling function in a perturbation expansion with respect to the effective coupling constant v. However, there are serious technical problems associated with the nonanalytical dependence of the shift of the percolation threshold p_c on u_0 [Eq. (3.15)]. This is, however, not a particular difficulty of our theoretical approach, but a fundamental problem for any field-theoretical calculation at fixed dimension below d_c. Schloms and Dohm [24] have shown that for a ϕ^4 theory the nonvanishing mass shift can be incorporated in the minimal subtraction approach directly in three dimensions without recourse to the standard $(\epsilon = 4 - d)$ expansion. But, even for this "standard model" of critical phenomena there does not exist a straightforward perturbation method at finite external momenta which allows for a consistent treatment of the nonanalytical mass shift at fixed dimension. Hence, at the present stage of the theory, we can treat the ζ functions to arbitrary loop order, but have to restrict ourselves to a mean-field (zero-loop) treatment for the scaling functions. Nevertheless, one expects that the results for the effective exponents obtained within this "renormalized mean-field theory" to provide a reasonably good approximation. This expectation is based on the experience that amplitude (or scal-

ing) functions are usually smooth and well behaved, and enter the results less sensitively than the exponential ζ functions. In fact, our approach was especially designed to incorporate the complete crossover behavior into the exponential functions ζ_a. This has to be contrasted with the usual scheme, where the crossover has to be inferred from high-order calculations of the amplitude functions (and usually does not go far beyond the determination of corrections to scaling).

The most convenient way to analyze the crossover behavior of the pair correlation function is in terms of effective critical exponents. We consider first the case $r = 0$ and $\mathbf{q} = 0$ and choose to define the effective critical exponent $\eta_{\parallel\,\mathrm{eff}}$ by [compare (4.19)]

$$2 - \eta_{\parallel\,\mathrm{eff}}(\omega) = \frac{d \ln \sqrt{|\,\Gamma_{11}(0,\mathbf{0},\omega)\,|^2}}{d \ln \omega}. \tag{4.42}$$

Using the matching condition

$$\left| \frac{\omega^2}{\mu^2 \ell^2 c^2(\ell)} + 2i \frac{\omega g(\ell)}{\mu \ell c(\ell)} \right|^2 = 1, \tag{4.43}$$

the effective exponent is found to be

$$2 - \eta_{\parallel\,\mathrm{eff}}(\ell) = [2 + \zeta_\phi(\ell)] \frac{d \ln \ell}{d \ln \omega}, \tag{4.44}$$

where the factor $d \ln \ell / d \ln \omega$ has to be determined from (4.43). The effective exponent $2 - \eta_{\parallel\,\mathrm{eff}}(\ell)$ is shown in Fig. 7 as a function of the flow parameter ℓ, where for the initial value $v(1) = v_{\mathrm{I}}^*$, and a series of initial values for the anisotropy parameter, $g(1) = 10^{-k}$ with $k = 2, 3, 4$, have been chosen. Upon using the matching condition (4.43) the flow parameter ℓ can be related to the longitudinal length scale ("frequency"). If the effective exponent is plotted versus the running anisotropy parameter $g(\ell)$, all the curves for different initial values $g(1)$ collapse onto one master curve. The corresponding plot is shown in Fig. 8. Since $g(\ell) \propto \ell^{\zeta_g^*}$ near a fixed point, the scale transformation (in order to reduce all curves to one master curve) depends on how close the flow is to one of the

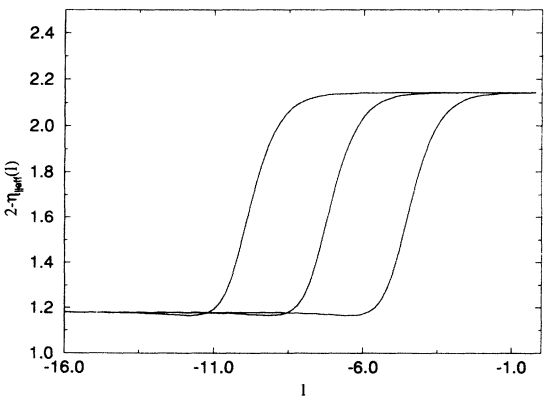

FIG. 7. Effective exponent $2 - \eta_{\parallel\,\mathrm{eff}}(\ell)$ for the connectivity as a function of the flow parameter ℓ for fixed initial values $v(1) = v_{\mathrm{I}}^*$ and a series of initial values for the anisotropy parameter [$g(1) = 10^{-2}$, 10^{-3}, and 10^{-4}].

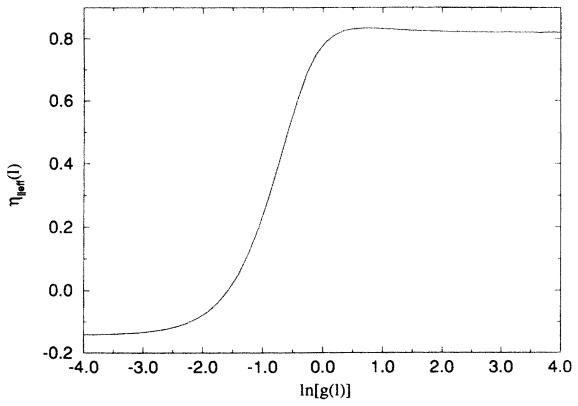

FIG. 8. Effective exponent $\eta_{\parallel\,\mathrm{eff}}(\ell)$ for the pair correlation function as a function of the running anisotropy parameter $g(\ell)$ for a fixed initial value of the coupling constant $v(1) = v_{\mathrm{I}}^*$.

four different fixed points. Note that because ζ_g is not a constant, no simple scaling relation can be deduced for the location of the crossover by simply investigating any one of the two asymptotic regimes.

Next, in the case $r = 0$ and $\omega = 0$ one can define an effective exponent $\eta_{\perp\,\mathrm{eff}}$ by [see Eq. (4.17)]

$$2 - \eta_{\perp\,\mathrm{eff}}(q) = \frac{d \ln \Gamma_{11}(0,\mathbf{q},0)}{d \ln q}. \tag{4.45}$$

With the matching condition $(q/\mu\ell)^2 = 1$ this reduces to

$$2 - \eta_{\perp\,\mathrm{eff}}(\ell) = 2 + \zeta_\phi(\ell). \tag{4.46}$$

Finally, we consider the case $\omega = 0$ and $\mathbf{q} = 0$. Upon defining an effective exponent [compare (4.21)]

$$\gamma_{\mathrm{eff}}(r) = \frac{d \ln \Gamma_{11}(r,\mathbf{0},0)}{d \ln r} \tag{4.47}$$

and choosing the matching condition $r(\ell) = 1$ we find

$$\gamma_{\mathrm{eff}}(\ell) = [2 + \zeta_\phi(\ell)] \frac{d \ln \ell}{d \ln r} = -\frac{2 + \zeta_\phi(\ell)}{\zeta_r(\ell)}; \tag{4.48}$$

remarkably, Eq. (4.48) is valid throughout the entire crossover region, and not just near one of the fixed points, where it becomes identical to the scaling relation (4.22).

The flows of the above effective exponents, and that of the "effective" dynamic exponent

$$z_{\mathrm{eff}}(\ell) = 1 + \zeta_c(\ell) - \zeta_g(\ell), \tag{4.49}$$

are shown in Figs. 8–11 versus the scaling variable $\ln[g(\ell)]$, with $\mu = 1$, and the initial value $v(1) = v_{\mathrm{I}}^*$, such that the universal crossover starting from the isotropic scaling region is described. The most important conclusion to be drawn from these results is that the characteristic anisotropy scales $g(\ell_{\mathrm{cross}})$, where the crossover occurs for the effective exponents defined above, are different. The effective exponent $\eta_{\parallel\,\mathrm{eff}}$ starts to cross over from the isotropic to the directed fixed point value already at $\ln g(\ell_{\mathrm{cross}}) \approx -0.8$, whereas the effective exponent γ_{eff} shows this crossover at $\ln g(\ell_{\mathrm{cross}}) \approx -0.1$, and the "dy-

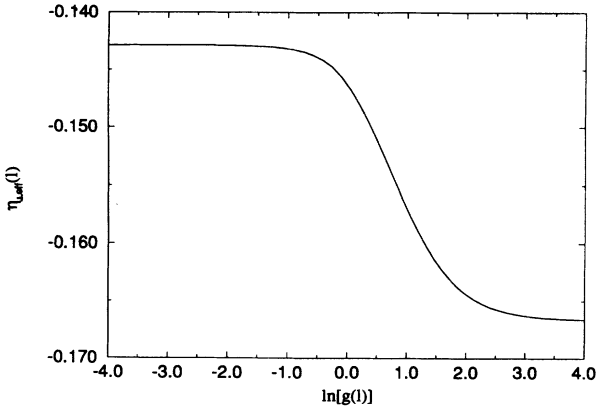

FIG. 9. Effective exponent $\eta_{\perp\,\mathrm{eff}}(\ell)$ for the pair correlation function as a function of the running anisotropy parameter $g(\ell)$ for a fixed initial value of the coupling constant $v(1) = v_{\mathrm{I}}^*$.

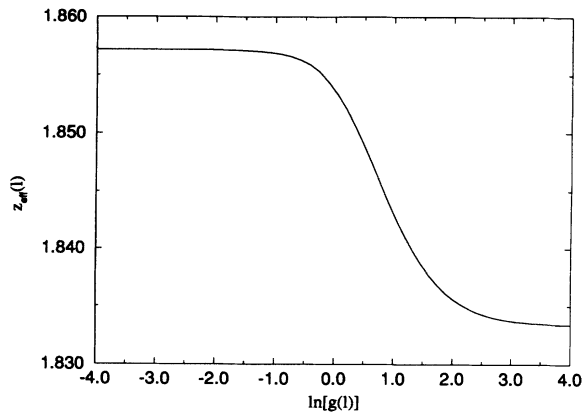

FIG. 11. Effective exponent $z_{\mathrm{eff}}(\ell)$, describing the anisotropy, as a function of the running anisotropy parameter $g(\ell)$ for a fixed initial value of the coupling constant $v(1) = v_{\mathrm{I}}^*$.

namical" exponent z_{eff}, as well as $\eta_{\perp\,\mathrm{eff}}$, at an even larger value $\ln g(\ell_{\mathrm{cross}}) \approx 0.8$. Note that the remarkable change of $\eta_{\parallel\,\mathrm{eff}}$ is already apparent at mean-field level, where it acquires the values 0 and 1 in the isotropic and directed limit, respectively. However, a description of the crossovers for $\eta_{\perp\,\mathrm{eff}}$, γ_{eff}, and z_{eff} requires the ζ functions as least on the one-loop level, as has been achieved here.

We remark that a precise calculation of these crossover features has not been possible up to this present work. Of course, the exponents for the limits of both isotropic and directed percolation have been determined to a much higher accuracy than is provided in our one-loop approximation [2–10]. In fact, the relative errors of our one-loop results, as compared to the values given in Table III of Ref. [3], are approximately 0.03, 0.09, and 0.21 for the exponent γ of directed percolation in $d = 4$, 3, and 2 dimensions, respectively, and for $\nu_\perp$ one finds correspondingly 0.10 and 0.27 for the three- and two-dimensional cases. In the isotropic limit at two dimensions, the relative errors are 0.21 and 0.27 for γ and ν, respectively.

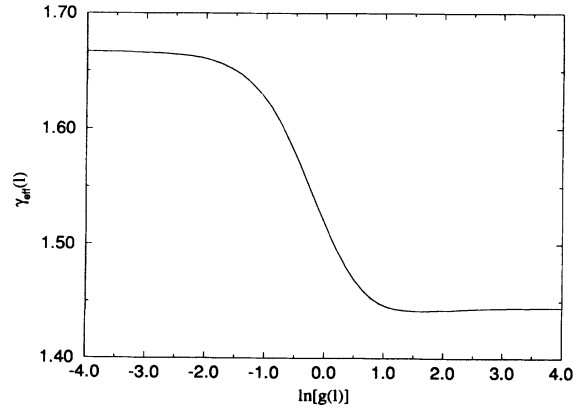

FIG. 10. Effective exponent $\gamma_{\mathrm{eff}}(\ell)$ for the connectivity as a function of the running anisotropy parameter $g(\ell)$ for a fixed initial value of the coupling constant $v(1) = v_{\mathrm{I}}^*$.

(We remark that the numerical values of our one-loop results are even slightly better than those of an additional ϵ expansion; yet they also improve as the upper critical dimension is approached.) However, our aim was rather to calculate the detailed crossover properties, and we believe that the characteristic crossover scales $g(\ell_{\mathrm{cross}})$ should not be affected too severely by, e.g., higher orders of perturbation theory. Certainly, these results, i.e., the approximations used in this paper, are subject to tests by both computer simulations and experiment. Of course, it would be very interesting to compare our predictions concerning the crossover scales of the different effective exponents with the outcome of such numerical simulations and/or physical experimental setups.

Therefore we add some remarks on the interpretation of our results, and on the number of free parameters of the theory. One of the advantages of studying the effective exponents is the fact that they do *not* depend on nonuniversal amplitudes, i.e., on the initial values $u(1)$, $c(1)$ (which can be set to 1, if one starts from the isotropic scaling region), and the scale μ. For convenience, we have plotted our results versus the scaling variable $\ln[g(\ell)]$ in Figs. 8–11, and have thus also eliminated the dependence on the formal anisotropy parameter. However, in simulations or experiments $g(1) = g$ is a fixed quantity, although its correspondence to a physical anisotropy measure may be rather indirect. In any case, if merely the *universal* crossover features are to be investigated, the initial value of the effective coupling should be chosen as $v(1) = v_{\mathrm{I}}^*$, in order to resemble the self-similar scaling behavior, and then $g(1)$ is the *only* free parameter of the theory. In order to compare directly with our figures, one then has to solve the flow equations (4.8), (4.14) with Eqs. (4.25)– (4.29), and apply the relevant matching condition, which is straightforward [unfortunately, the scaling behavior with respect to $g(1)$ is complex and cannot be described by a pure power law). But once $g(1)$ has been determined for one of the effective exponents, it must necessarily also yield the crossover point for any of the others. Obviously, a quantitative study of the effective indices $\eta_{\parallel\,\mathrm{eff}}(\omega)$ and $\gamma_{\mathrm{eff}}(r)$ is most promising, while

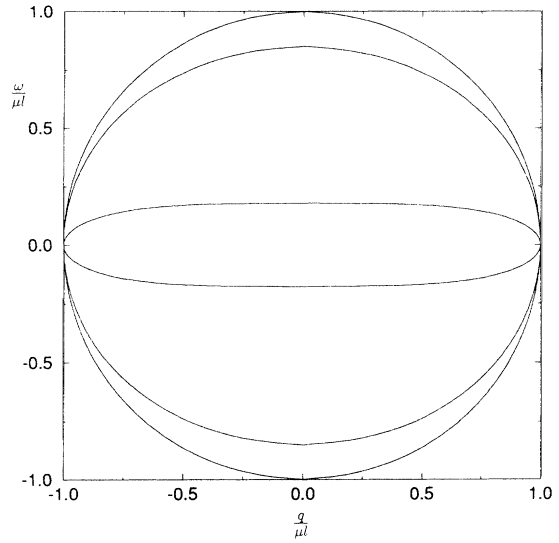

FIG. 12. Contour plots for $\Gamma_{11}(0,\mathbf{q},\omega)$, as inferred from Eqs. (4.50) and (4.51), with values of $\ell = 10^{-4}$, 10^{-3}, and 10^{-2}, respectively.

a detailed analysis of $\eta_{\perp\,\mathrm{eff}}(q)$ and $z_{\mathrm{eff}}(\ell)$ is probably difficult, because of their comparatively small changes on approaching the self-affine regime.

Possibly clearer on first sight, however somewhat less distinct concerning quantitative features, is a discussion of the crossover from self-similar to self-affine scaling on the basis of contour plots, e.g., for $\Gamma_{11}(0,\mathbf{q},\omega)$. Applying the matching condition

$$\left|\frac{q^2}{\mu^2\ell^2} + \frac{\omega^2}{\mu^2\ell^2 c(\ell)^2} + 2i\frac{\omega g(\ell)}{\mu\ell c(\ell)}\right| = 1, \tag{4.50}$$

valid at the percolation threshold $p = p_c$, Eq. (4.41) simply becomes

$$\Gamma_{11}(0,\mathbf{q},\omega) = \mu^2\ell^2 e^{\int_1^\ell \zeta_\phi(\ell')d\ell'/\ell'}, \tag{4.51}$$

which is a monotonic function of ℓ (the exponential is approximately given by $\ell^{-\eta_{\perp\,\mathrm{eff}}(\ell)}$; see Fig. 9). Therefore, contours of constant Γ_{11} are identical to contours of constant flow parameter ℓ, which in turn can be easily inferred from Eq. (4.50). In Fig. 12, we depict typical examples of such contour plots, with values of $\ell = 10^{-4}$, 10^{-3}, and 10^{-2}, respectively, from which the crossover from isotropic to anisotropic scaling becomes apparent.

V. SUMMARY AND CONCLUSION

In this paper we have investigated the crossover from isotropic to directed percolation taking advantage of a mapping onto a field-theoretical representation of the connectivity [4, 8]. From a conceptual point of view, the main result of the present paper is the demonstration that an extended minimal subtraction scheme is capable of dealing with crossover problems associated with a change in the upper critical dimension d_c in the framework of renormalization-group theory. We have exemplified the method for a long standing problem in percolation theory. But we believe that this approach can be applied to a wide variety of interesting physical problems. Among those of most current interest are the crossover between bulk and surface physics [26], between mean-field and critical behavior [21], crossover from propagating to overdamped soft modes in critical dynamics, e.g., near structural phase transitions, and others.

Since our primary goal was to present the formalism, we have restricted ourselves to a one-loop approximation. We have identified the crossover exponent Δ and calculated effective exponents for different length scales and the pair correlation function. Higher loop orders for the exponential (ζ) functions are in principle accessible within our theoretical framework. However, the calculation of the wave vector and frequency dependence of the amplitude functions and the incorporation of the non-analytical mass shift remains an open problem for a field theoretical calculation at fixed dimension [24].

It would also be interesting to investigate the crossover from isotropic to directed percolation by numerical simulations or physical experiments, and compare them with the theoretical results of our paper. Even though the values of the critical exponents in the two asymptotic regimes are not accurate (one-loop results), we expect the crossover behavior of the effective exponents to be qualitatively correct. Especially the predictions concerning the different loci of the crossover for the "static" and "dynamic" quantities could be tested by numerical simulations. Obviously, this would be of considerable help for estimating the quality of the proposed approach to crossover phenomena also in different situations, where a numerical simulation is either very cumbersome or not feasible at all.

ACKNOWLEDGMENTS

We would like to thank S. Clar, who simulated the percolation clusters of Fig. 1. We gratefully acknowledge support from the Deutsche Forschungsgemeinschaft (DFG) under Contracts No. Fr. 850/2-1 and No. Schw. 348/4-2.

APPENDIX A: TWO- AND THREE-POINT VERTEX FUNCTIONS TO ONE-LOOP ORDER

For the sake of completeness, we list some important explicit analytical results for the two- and three-point vertex functions to one-loop order. The corresponding Feynman diagrams are depicted in Fig. 4. Writing the free propagator in the form

$$G^0_{11\,(0)}(-\mathbf{q},-\omega) = \frac{c_0^2}{[\omega-\omega_+(\mathbf{q})][\omega-\omega_-(\mathbf{q})]}, \tag{A1}$$

where $\omega_\pm(\mathbf{q})$ represents the "dispersion relation" for the "elementary excitations" of our model,

$$\omega_\pm(\mathbf{q}) = -ic_0\left(g_0 \mp \sqrt{r_0 + g_0^2 + q^2}\right), \tag{A2}$$

one finds for $\Gamma^0_{11}(\mathbf{q},\omega)$:

$$(a) = r_0 + q^2 + \omega^2/c_0^2 + 2g_0 i\omega/c_0, \tag{A3}$$

$$(b) = \frac{u_0^2 c_0^4}{2} \int_k \int_\nu G^0_{11\,(0)}(\mathbf{k}-\mathbf{q}/2, \nu-\omega/2) G^0_{11\,(0)}(\mathbf{k}+\mathbf{q}/2, \nu+\omega/2) \tag{A4}$$

$$= u_0^2 c_0^5 \int_k \frac{1}{\sqrt{r_0 + g_0^2 + (\mathbf{q}/2-\mathbf{k})^2}} \frac{(\mathbf{qk}) + \omega^2/2c_0^2 + 2g_0 i\omega/c_0 - 2g_0^2}{[-\omega + \omega_+(\mathbf{q}/2+\mathbf{k}) + \omega_+(\mathbf{q}/2-\mathbf{k})]\,[-\omega + \omega_-(\mathbf{q}/2+\mathbf{k}) + \omega_+(\mathbf{q}/2-\mathbf{k})]}$$
$$\times \frac{1}{[-\omega + \omega_+(\mathbf{q}/2+\mathbf{k}) + \omega_-(\mathbf{q}/2-\mathbf{k})]\,[-\omega + \omega_-(\mathbf{q}/2+\mathbf{k}) + \omega_-(\mathbf{q}/2-\mathbf{k})]}\,. \tag{A5}$$

In the last step, we have performed the integration over the internal frequency ν via the residue theorem.

As a special case, we list the result for vanishing external wave vector, $\mathbf{q} = 0$, which enters the calculation of the effective exponents:

$$\Gamma^0_{11}(\mathbf{0}, \omega) = r_0 + \frac{\omega^2}{c_0^2} + 2g_0 \frac{i\omega}{c_0} + \frac{u_0^2 c_0}{8} \int_k \frac{1}{\sqrt{r_0 + g_0^2 + k^2}} \frac{1}{r_0 + k^2 + \frac{\omega^2}{4c_0^2} + g_0 \frac{i\omega}{c_0}}. \tag{A6}$$

In order to calculate the renormalization constants, we may expand (A5) with respect to q^2 and ω:

$$\Gamma^0_{11}(\mathbf{q}, \omega) = r_0 \left(1 + \frac{u_0^2 c_0}{8 r_0} \int_k \frac{1}{\sqrt{r_0 + g_0^2 + k^2}(r_0 + k^2)}\right)$$
$$+ 2g_0 \frac{i\omega}{c_0} \left(1 - \frac{u_0^2 c_0}{16} \int_k \frac{1}{\sqrt{r_0 + g_0^2 + k^2}(r_0 + k^2)^2}\right)$$
$$+ \frac{\omega^2}{c_0^2} \left(1 - \frac{u_0^2 c_0}{32} \int_k \frac{1}{\sqrt{r_0 + g_0^2 + k^2}(r_0 + k^2)^2} - \frac{u_0^2 c_0 g_0^2}{8} \int_k \frac{1}{\sqrt{r_0 + g_0^2 + k^2}(r_0 + k^2)^3}\right)$$
$$+ q^2 \left(1 - \frac{u_0^2 c_0}{32} \int_k \frac{1}{\sqrt{r_0 + g_0^2 + k^2}(r_0 + k^2)^2} - \frac{u_0^2 c_0}{64} \int_k \frac{1}{\sqrt{(r_0 + g_0^2 + k^2)^3}(r_0 + k^2)}\right)$$
$$+ \frac{u_0^2 c_0}{32} \int_k \frac{(\mathbf{qk})^2}{\sqrt{(r_0 + g_0^2 + k^2)^3}(r_0 + k^2)^2} + \frac{3u_0^2 c_0}{64} \int_k \frac{(\mathbf{qk})^2}{\sqrt{(r_0 + g_0^2 + k^2)^5}(r_0 + k^2)} + \mathcal{O}(\omega^3, q^4). \tag{A7}$$

Similarly, the three-point vertex function $\Gamma^0_{12}(-\mathbf{q}, -\omega; \mathbf{q}/2, \omega/2; \mathbf{q}/2, \omega/2)$ reads

$$(c) = -u_0/2, \tag{A8}$$

$$(d) = u_0^3 c_0^6 \int_k \int_\nu G^0_{11\,(0)}(\mathbf{k}-\mathbf{q}/2, \nu-\omega/2) G^0_{11\,(0)}(\mathbf{k}+\mathbf{q}/2, \nu+\omega/2) G^0_{11\,(0)}(\mathbf{k}, \nu) \tag{A9}$$

$$= \frac{u_0^3 c_0^5}{2} \int_k \Bigg[\frac{1}{\sqrt{r_0 + g_0^2 + (\mathbf{q}/2+\mathbf{k})^2}} \frac{1}{[-\omega + \omega_+(\mathbf{q}/2+\mathbf{k}) + \omega_+(\mathbf{q}/2-\mathbf{k})]\,[-\omega + \omega_+(\mathbf{q}/2+\mathbf{k}) + \omega_-(\mathbf{q}/2-\mathbf{k})]}$$
$$\times \frac{1}{[-\omega/2 + \omega_+(\mathbf{q}/2+\mathbf{k}) - \omega_+(\mathbf{k})]\,[-\omega/2 + \omega_+(\mathbf{q}/2+\mathbf{k}) - \omega_-(\mathbf{k})]}$$
$$+ \frac{1}{\sqrt{r_0 + g_0^2 + (\mathbf{q}/2-\mathbf{k})^2}} \frac{1}{[-\omega + \omega_+(\mathbf{q}/2+\mathbf{k}) + \omega_-(\mathbf{q}/2-\mathbf{k})]\,[-\omega + \omega_-(\mathbf{q}/2+\mathbf{k}) + \omega_-(\mathbf{q}/2-\mathbf{k})]}$$
$$\times \frac{1}{[-\omega/2 + \omega_-(\mathbf{q}/2-\mathbf{k}) + \omega_+(\mathbf{k})]\,[-\omega/2 + \omega_-(\mathbf{q}/2-\mathbf{k}) + \omega_-(\mathbf{k})]}$$
$$+ \frac{1}{\sqrt{r_0 + g_0^2 + k^2}} \frac{1}{[-\omega/2 + \omega_+(\mathbf{q}/2+\mathbf{k}) - \omega_+(\mathbf{k})]\,[-\omega/2 + \omega_-(\mathbf{q}/2+\mathbf{k}) - \omega_+(\mathbf{k})]}$$
$$\times \frac{1}{[-\omega/2 + \omega_+(\mathbf{q}/2-\mathbf{k}) + \omega_-(\mathbf{k})]\,[-\omega/2 + \omega_-(\mathbf{q}/2-\mathbf{k}) + \omega_-(\mathbf{k})]} \Bigg]. \tag{A10}$$

For the determination of the renormalization constant Z_u, however, we merely need

$$\Gamma^0_{12}(\mathbf{0}, 0; \mathbf{0}, 0; \mathbf{0}, 0) = -\Gamma^0_{21}(\mathbf{0}, 0; \mathbf{0}, 0; \mathbf{0}, 0)$$

$$= -\frac{u_0}{2} \left(1 - \frac{u_0^2 c_0}{4} \int_k \frac{1}{\sqrt{r_0 + g_0^2 + k^2}(r_0 + k^2)^2} - \frac{u_0^2 c_0}{8} \int_k \frac{1}{\sqrt{(r_0 + g_0^2 + k^2)^3}(r_0 + k^2)}\right). \tag{A11}$$

APPENDIX B: FEYNMAN PARAMETER INTEGRALS

Within the generalized minimal subtraction scheme described above, the determination of the Z factors after performing the frequency and momentum integration using the Feynman parametrization

$$\frac{1}{A^r B^s} = \frac{\Gamma(r+s)}{\Gamma(r)\Gamma(s)} \int_0^1 \frac{x^{r-1}(1-x)^{s-1}}{[xA+(1-x)B]^{r+s}} dx \quad \text{(B1)}$$

[$\Gamma(x)$ is Euler's gamma function] leads to integrals of the form (with odd integers m, n)

$$I^d_{mn}(g) = \int_0^1 \frac{x^{m/2-1}}{(1+xg^2)^{(m+n-d)/2}} dx = g^{-m} \int_0^{g^2} \frac{t^{m/2-1}}{(1+t)^{(m+n-d)/2}} dt, \quad \text{(B2)}$$

for which one may immediately derive asymptotic relations for $g = 0$ and $g \to \infty$, respectively [$B(x,y) = \Gamma(x)\Gamma(y)/\Gamma(x+y)$ denotes Euler's beta function],

$$I^d_{mn}(0) = 2/m, \quad \text{(B3)}$$

$$\lim_{g\to\infty} \left[g^m I^d_{mn}(g)\right] = B\left(\frac{m}{2}, \frac{n-d}{2}\right) = \frac{\Gamma(\frac{m}{2})\Gamma(\frac{n-d}{2})}{\Gamma(\frac{m+n-d}{2})}. \quad \text{(B4)}$$

For the calculation of the ζ functions, the following formulas are very useful:

$$I^d_{mn}(g) - g^2 I^d_{m+2,n}(g) = I^d_{m,n+2}(g), \quad \text{(B5)}$$

$$\mu \frac{\partial}{\partial \mu} I^d_{mn}(g_0/\mu) = (m+n-d)\frac{g_0^2}{\mu^2} I^d_{m+2,n}(g_0/\mu). \quad \text{(B6)}$$

[1] B. B. Mandelbrot, *The Fractal Geometry of Nature* (Freeman, San Francisco, 1982); J. Feder, *Fractals* (Plenum, New York, 1988).

[2] For a review on the theory of percolation, see J. W. Essam, Rep. Prog. Phys. **43**, 834 (1980); D. Stauffer and A. Aharony, *Introduction to Percolation Theory*, 2nd ed. (Taylor and Francis, London, 1992).

[3] For a review, see W. Kinzel, in *Percolation Structures and Processes*, Annals of the Israel Physical Society Vol. 5, edited by G. Deutscher, R. Zallen, and J. Adler (Bar-Ilan University, 1983), p. 425.

[4] J. L. Cardy and R. L. Sugar, J. Phys. A **13**, L423 (1980).

[5] R. Brower, M. A. Furman, and K. Subbarao, Phys. Lett. B **78** , 213 (1978).

[6] M. Henkel and H. J. Herrmann, J. Phys. A **23**, 3719 (1990).

[7] P. Grassberger, J. Phys. A **22**, 3673 (1989).

[8] J. Benzoni and J. L. Cardy, J. Phys. A **17**, 179 (1984).

[9] P. Grassberger and A. De La Torre, Ann. Phys. (N.Y.) **122**, 373 (1979).

[10] J. Benzoni, J. Phys. A **17**, 2651 (1984).

[11] S.P. Obukhov, Physica A **101**, 145 (1980).

[12] N. Van Lieu and B. I. Shklovskii, Solid State Commun. **38**, 99 (1981).

[13] J. Kertész and T. Vicsek, J. Phys. C **13**, L343 (1980).

[14] P. Grassberger, J. Phys. A **18**, L215 (1985).

[15] H. K. Janssen, Z. Phys. B **23**, 377 (1976); R. Bausch, H. K. Janssen, and H. Wagner, *ibid.* **24**, 113 (1976).

[16] D. J. Amit and Y. Y. Goldschmidt, Ann. Phys. (N.Y.) **114**, 356 (1978).

[17] D. J. Amit, *Field Theory, the Renormalization Group, and Critical Phenomena*, 2nd ed. (World Scientific, Singapore, 1984).

[18] I. D. Lawrie, J. Phys. A **14**, 2489 (1981); **18**, 1141 (1985).

[19] E. Frey and F. Schwabl, J. Phys. (Paris) Colloq. **48**, C8-1569 (1988); Phys. Rev. B **42**, 8261 (1990); **43**, 833 (1991).

[20] U. C. Täuber and F. Schwabl, Phys. Rev. B **46**, 3337 (1992).

[21] U. C. Täuber and F. Schwabl, Phys. Rev. B **48**, 186 (1993).

[22] G. t'Hooft and M. Veltman, Nucl. Phys. B **44**, 189 (1972).

[23] However, in the usual ϵ expansion scheme, which constitutes a well-defined perturbation approach provided that $\epsilon \ll 1$, one finally has to insert values $\epsilon = 1$, or even $\epsilon = 2$ or 3 in the case of directed and isotropic percolation, respectively, in order to describe the cricital behavior in $d = 3$ dimensions.

[24] R. Schloms and V. Dohm, Nucl. Phys. B **328**, 639 (1989); Phys. Rev. B **42**, 6142 (1990).

[25] In most of the literature on directed percolation [4] there is, unfortunately, a different definition for the critical exponents $\tilde{\eta}_\parallel$ and $\tilde{z}$. The relation to our definition is $\tilde{\eta}_\parallel = 1 - \eta_\parallel$ and $\tilde{z} = z/2$. Our definition of the critical exponents corresponds to the usual convention used in the theory of static and dynamic critical phenomena.

[26] H. W. Diehl, in: *Phase Transitions and Critical Phenomena*, edited by C. Domb and J. L. Lebowitz (Academic, London, 1986), Vol. 10, p. 75.